CTH-IEFT/PP-1990-19 ISSN

MODELLING OF PROMPT LOSSES OF HIGH ENERGY CHARGED PARTICLES IN TOKAMAKS

Ö. Dillner, D. Anderson, H. Hamnén, and M. Lisak

INSTITUTIONEN FÖR ELEKTROMAGNETISK FÄLTTEORI

CHALMERS TEKNISKA HÖGSKOLA

CTH-IEFT/PP-1990-19

Modelling of prompt losses of high energy charged particles in Tokamaks

Ö. Dillner, D. Anderson, H. Hamnen, and M. Lisak

Institute for Electromagnetic Field Theory
Chalmers University of Technology
S-41296 Göteborg Sweden

ABSTRACT

A simple analytical expression for the total prompt loss fraction of high energy charged particles in an axisymmetric Tokamak is derived. The results are compared with predictions obtained from numerical simulations and show good agreement. An application is made to sawtooth induced changes in the losses of fusion generated high energy charged particles. Particular emphasis is given to the importance of (i) sawtooth induced profile changes of the background ion densities and temperature as well as to (ii) redistribution of particles which have accumulated during the sawtooth rise but are being lost by redistribution at the sawtooth crash.

1. INTRODUCTION

In a future DT Tokamak fusion reactor, the energy balance is established as a competition between the power loss from the plasma and the power deposition heating from the fusion generated 3.5 MeV alpha particles. In order to facilitate ignition and a subsequent self-sustained burn, it is important that the alpha particles are confined long enough to transfer most of their energy to the plasma before being lost.

The most fundamental loss mechanism of high energy alpha particles is prompt losses due to guiding center orbits intersecting the vessel wall within a bounce time [1]. Obviously, the fraction of promptly lost high energy alphas is an important input parameter in the analysis of the energy balance of a future Tokamak fusion reactor, although stochastic banana orbit diffusion caused by the toroidal magnetic field ripple often may be an even more serious loss mechanism [2]. However, the confinement properties of high energy charged particles in general also have important applications e.g. to wall loading due to blistering from lost high energy charged particles [3] burn-up studies [4] high energy particles created by ICRF heating and neutral beam heating [5], and sawtooth and/or MHD-induced particle losses [6, 7].

Many investigations of prompt alpha particle losses have been based on numerical codes, e.g. [8], which often are too cumbersome for routine use in situations where the prompt loss itself is not the goal, but only the means to evaluate other quantities. Some analytical investigations have also been made e.g. [9-11], which however tend to result in estimates rather than accurate predictions for the prompt loss fraction.

In the present work we will derive a simple and useful formula for the fraction of promptly lost high energy charged particles in an axisymmetric Tokamak plasma. The situation of moderate prompt losses is emphasized, since present JET-sized and future NET/ITER-sized Tokamaks are good containers of high energy charged particles. The accuracy of the formula is demonstrated to be good by comparisons with computer results obtained by the CASINO code.

The resulting approximation for the prompt particle losses is then used to analyze the sawtooth induced variation of fusion generated alpha particle losses. Two mechanisms affecting the loss rate at the sawtooth crash are discussed: (i) changes in background ion density and temperature and (ii) redistribution of accumulated alpha particles into unconfined orbits. The first mechanism gives a drop in loss burst similar to what is observed in other quantities e.g. density, temperature etc. whereas the latter mechanism gives

rise to a short but intensive loss burst during the redistribution time following the sawtooth crash.

2. BACKGROUND

The guiding centers of charged particles moving along the curved field lines in a Tokamak magnetic field, tend to deviate from the flux surfaces on which they are born, as a result of radial drifts due to the curvature and the gradient of the magnetic field.

The largest deviations occur for trapped particles, which trace out banana orbit projections in the poloidal cross section with a width, δ, given by

$$\delta = 2\frac{mv_{\|m}}{ZeB_p} \tag{1}$$

where B_p, the poloidal component of the magnetic field, is directly determined by the magnitude and profile of the current, m and Z are the mass and charge number respectively of the particle, and $v_{\|m}$ is the maximum parallel velocity in the orbit. Eq. (1) for the banana width can be reformulated to give the following estimate

$$\delta \simeq \frac{2\sqrt{2}q}{\sqrt{\varepsilon}}\rho_L \tag{2}$$

where q is the safety factor, ε is the inverse of the aspect ratio A, and ρ_L is the Larmor radius of the particle in the toroidal field. Eq. (2) can be used to establish a qualitative criterion for good particle confinement by requiring e.g. $\delta(r=a/2) < a$, where a is the plasma minor radius. Assuming a parabolic current profile, this condition can be expressed as, [2]

$$I > \frac{3}{\sqrt{A}} \quad \text{MA} \tag{3}$$

where I denotes total plasma current. Thus e.g. for an aspect ratio $A \simeq 3$ (cf TFTR where $A \simeq 245/80$) we expect good confinement if $I > 1.7$ MA. Although eq. (3) provides a qualitative estimate of the requirements needed to confine a significant fraction of the fusion produced 3.5 MeV alphas, quantitative predictions must be based on a more detailed analysis of the particle orbit dynamics.

The topology of high energy particle orbits depends on the particle energy but also significantly on the pitch-angle of the particle at the point of birth. This is illustrated in Fig. 1, using results obtained by the CASINO code. A particle is considered lost when its orbit intersects the wall, i.e. when its distance from the plasma center, r, is larger than plasma minor radius, a, at some point in the orbit. Let r_b denote the radius where the particle is produced. Obviously, for high enough currents, there exists a critical radius, r_{bs} , which depends on current, and such that no prompt losses will occur for particles with $r_b < r_{bs}$.

The first particle to be lost is the counter-streaming particle with the largest banana width. This corresponds to the barely trapped orbit which is tangent to the limiter at the poloidal angle $\theta=0$. Since the particles produced in the equatorial plane deviate most from their radii of birth, it is of special interest to consider the loss region in velocity space for particles produced at $\theta=0$. This variation of loss region with birth radius is illustrated in Fig. 2. Increasing r_b above r_{bs} , more deeply trapped particles will hit the limiter and the loss region broadens. Finally, when r_b becomes larger than a critical radius, r_{bu}, the outer most of the passing particle orbits begin to intersect the limiter and the loss region increases dramatically.

Several attempts have been made to give simple models for the characteristic properties of the loss region, cf [1, 8, 9, 10] and Fig. 3. In the present work we will derive a simple but very accurate formula for the prompt losses which also incorporates the additional effect of particles being born at arbitrary poloidal angles.

3. ANALYSIS

3.1 Basic relations

Our analytical analysis is based on the method of constants of motion in a tokamak where the field geometry is assumed to be toroidally symmetric with concentric circular flux surfaces. The particles can be produced anywhere in the tokamak cross-section and the subscript b will be used to indicate coordinates, velocity components etc. at the moment of birth. The true motion of the particles is reduced to guiding centre orbits and the interaction with the bulk plasma is considered as negligible during a bounce time. Under these conditions, the canonical angular momentum, P_φ as well as the energy, E, and the magnetic moment, μ, will be preserved, i.e.

$$\mu = \frac{m v_\perp^2}{2B} = \text{constant}$$

$$E = \frac{m}{2}(v_\parallel^2 + v_\perp^2) = \text{constant}$$

$$P_\varphi = mRv_\parallel + ZeR_o A_\varphi = \text{constant} \tag{4}$$

where B denotes the toroidal magnetic field, $v_\perp$ the perpendicular velocity of the particle, $R=r+R_o$ with R_o being major radius, and A_φ is the toroidal component of the vector potential. Assuming the plasma current profile, J(r), to be modelled as

$$J(r) \propto \left[1-\left(\frac{r}{a}\right)^n\right]^p \tag{5}$$

where n and p are non-negative integers, we have the relation

$$A_\varphi = \frac{\mu_o I}{2\pi} F\left(\frac{r}{a}\right) \tag{6}$$

where I is the total current and F(x) is the normalized poloidal flux function given by

$$F(x) = \frac{\sum_{j=0}^{p} \frac{(-1)^j x^{nj+2}}{(nj+2)^2} \binom{p}{j}}{\sum_{j=0}^{p} \frac{(-1)^j}{(nj+2)} \binom{p}{j}} \tag{7}$$

From the conservation of the magnetic moment we obtain

$$\frac{v_\perp^2}{B} = \frac{v^2}{B_o}\frac{R_b}{R_o}\sin^2\chi_b \tag{8}$$

where χ denotes the pitch angle of the particle. Eq. (8) together with the conservation of energy implies

$$v_\parallel = \pm v\left(1-\frac{R_b}{R}\sin^2\chi_b\right)^{\frac{1}{2}} \tag{9}$$

and finally, eq. (9) together with the conservation of angular momentum yields

$$F\left(\frac{r}{a}\right) \pm P\left[\frac{R}{a^2}(R-R_b\sin^2\chi_b)\right]^{\frac{1}{2}} = F\left(\frac{r_b}{a}\right) \pm P\frac{R_b}{a}\cos\chi_b \tag{10}$$

where

$$P = \frac{2\pi m v}{ZeA\mu_o I} \tag{11}$$

and $A=R_o/a$ is the inverse aspect ratio.

3.2 Loss boundary characteristics

In order to simplify notations we introduce the normalization $r/a \rightarrow r$ and $R/a \rightarrow R$. The vertex point of the loss region, cf Figs. 2 and 3, corresponds to the limiting orbit between trapped and untrapped counter going particles which is tangential to the limiter at r=1. The turning point ($v_{//}=0$) of the corresponding banana orbit occurs approximately halfway between the innermost and outmost flux surfaces, i.e.

$$R_{v_{//}=0} \approx R_o - 1 + \frac{1}{2}(R_o+1-R_b) \tag{12}$$

which using eq. (9) implies

$$\cos^2\chi_b = \frac{1+3R_b-3R_o}{2R_b} \tag{13}$$

The radial excursion of the particle can then be determined by substituting eq. (13) into eq. (10). This yields

$$F(r) \pm P\sqrt{R(2R-3R_o+1+R_b)} = F(r_b) + P\sqrt{\frac{R_b(3R_b-3R_o+1)}{2}} \tag{14}$$

The situation when the fattest banana orbit just touches the outer wall ($R=R_o+1$, r=1) can be expressed as a condition on P, viz.

$$P = P_s(r_b) = \sqrt{\frac{2}{A}} \frac{F(1)-F(r_b)}{\left[\left(1+\frac{r_b}{A}\right)(1+3r_b)\right]^{\frac{1}{2}} + \left[\left(1+\frac{1}{A}\right)(3+r_b)\right]^{\frac{1}{2}}} \tag{15}$$

Using eqs. (11) and (15) the particle energy, E_s, corresponding to the vertex point of the loss region can be written

$$E_s(r_b) = \frac{1.93}{M} [ZAIP_s(r_b)]^2 \tag{16}$$

where M is the mass number of the particle and I is the total current in MA.

E_s decreases monotonically for increasing r_b and at the ends of the interval we have

$$E_s(0) = \frac{3.86\ A}{M}\left[\frac{ZIF(1)}{1+\sqrt{3\left(1+\frac{1}{A}\right)}}\right]^2$$

$$E_s(1) = 0 \tag{17}$$

An analytical approximation for $E_s(r_b)$ that exhibits the correct asymptotic behaviour at the terminal points can be given as

$$\sqrt{\frac{E_s(r_b)}{E_s(0)}} = (1-\beta)r_b^3 - 2(1-\beta)r_b^2 - \beta r_b + 1 \tag{18}$$

where

$$\beta = \frac{3\left(3+\frac{1}{A}\right)+\sqrt{3\left(1+\frac{1}{A}\right)}}{6\left[1+\sqrt{3\left(1+\frac{1}{A}\right)}\right]}$$

The second characteristic energy of the velocity space loss region is the particle energy corresponding to the limiting case when the loss region widens to include also passing counter-streaming particles.
According to Fig. 3, this energy is determined by the condition that a particle with initial pitch angle $\chi_b = \pi$ hits the limiter, i.e. from eq. (10)

$$F(1) + P(R_o-1) = F(r_o) + P(R_o+r_b) \tag{19}$$

which implies

$$P = P_u(r_b) = \frac{F(1) - F(r_b)}{1 + r_b} \tag{20}$$

The corresponding particle energy, $E_u(r_b)$ is then

$$E_u(r_b) = \frac{1.93}{M}(ZAIP_u)^2 \tag{21}$$

At the ends of the r_b-interval we have

$$E_u(0) = \frac{1.93}{M}[\,ZAIF(1)\,]^2$$
$$E_u(1) = 0 \tag{22}$$

and the intermediate variation of $E_u(r_b)$ can be approximated similarly to eq. (18).

$$\sqrt{\frac{E_u(r_b)}{E_u(0)}} \approx (\sigma-1)r_b^3 - (\sigma-1)r_b^2 - r_b + 1 \tag{23}$$

where the parameter σ depends on the current profile according to

$$\sigma = 2 - \frac{1}{2F(1)} \tag{24}$$

Note that $E_u > E_s$.

3.3 Approximation of characteristic loss radii

The importance of the prompt losses is determined by the magnitude of the particle energy, E, relative to the energies E_s and E_u , which characterize the velocity space loss region. Obviously, for particle energies $E < E_s < E_u$ no prompt losses will occur. The critical radius, r_{bs}, at which the first orbit loss occurs is determined from the condition

$$E_s(r_{bs}) = E \tag{25}$$

Using this in eq. (18) we obtain the simple approximation

$$r_{bs} = \left(1-\frac{1}{K_s}\right)^2 + \frac{1}{K_s}\left\{\left[1+3\left(1-\frac{1}{K_s}\right)\right]^{\frac{1}{2}} - 1\right\} \tag{26}$$

where

$$K_s = \left(\frac{A}{ME}\right)^{\frac{1}{2}} \frac{2\,ZIF(1)}{1+\sqrt{3\left(1+\frac{1}{A}\right)}} \tag{27}$$

and E is expressed in MeV. In Figs. 4 and 5 are shown r_{bs} as a function of K_s and K_s as a function of the current profile exponent p for n=2.

Analogously we obtain for the critical radius, r_{bu}, where passing particles begin to be lost

$$r_{bu} = \left(1-\frac{1}{K_u}\right)\left\{\frac{1}{K_u} + \frac{\sigma}{2(\sigma-1)} - \left[\frac{\sigma^2}{4(\sigma-1)^2} - \frac{1-\frac{1}{K_u}}{\sigma-1}\right]^{\frac{1}{2}}\right\} \tag{28}$$

where

$$K_u = \frac{1.4\,ZAIF(1)}{\sqrt{ME}} \tag{29}$$

3.4 Local loss fraction

Having established the characteristic features of the loss region, we proceed to derive a model for the local loss fraction $l(r_b,\theta_b)$, i.e. the relative number of particles being born at (r_b,θ_b) in the poloidal plane and lost during a bounce time.

The modelling rests on the following observations and approximations:

(i) no losses occur for $r_b < r_{bs}$.

(ii) for $r_{bs} < r_b < r_{bu}$, the fraction of lost trapped particles increases approximately linear from zero to $\alpha_T(\theta)$ at $r_b=1$, where $\alpha_T(\theta)$ denote the total fraction of trapped

particles.

(iii) for $r_{bu} < r_b$, all passing counter streaming particles are considered lost.

A counter streaming particle born at the limiter $(1,\theta_b)$ and on the boundary between trapped and untrapped particles will have an initial pitch angle $\chi_*(\theta_b)$ determined by

$$\sin^2\chi_*(\theta_b) = \frac{v_{\perp b}^2}{v^2} = \frac{v_{\perp b}^2}{v_{\perp\theta=\pi}^2} = \frac{B(\theta_b)}{B(\pi)} = \frac{1-\frac{\cos\theta_b}{A}}{1+\frac{1}{A}} \tag{30}$$

The pitch angle, χ, of trapped counter streaming particles produced at $(1,\theta_b)$ must then satisfy

$$\chi_*(\theta_b) \le \chi \le \frac{\pi}{2} \tag{31}$$

Thus an estimate of the fraction α_T of trapped counter streaming particles produced at the limiter can be written

$$\alpha_T(\theta_b) = \frac{1}{2}\int_{\chi_*}^{\frac{\pi}{2}} \sin\chi'\, d\chi' = \frac{1}{2}\left(\frac{1+\cos\theta_b}{1+A}\right)^{\frac{1}{2}} \tag{32}$$

The fraction $\alpha_p(\theta_b)$ of passing counter streaming particles is then

$$\alpha_p(\theta_b) = \frac{1}{2} - \alpha_T(\theta_b) \tag{33}$$

Thus, finally we obtain the following approximation for the local loss fraction $l(r_b,\theta_b)$

$$l(r_b,\theta_b) = \begin{cases} 0 & 0 \le r_b \le r_{bs} \\ \alpha_T(\theta_b)\dfrac{r_b - r_{bs}}{1-r_{bs}} & r_{bs} \le r_b \le r_{bu} \\ \alpha_T(\theta_b)\dfrac{r_b - r_{bs}}{1-r_{bs}} + \alpha_p(\theta_b) & r_{bu} \le r_b \le 1 \end{cases} \tag{34}$$

3.5 Total loss fraction

Assuming a source profile for the produced particles according to

$$s(r) = s(0)\,[1-r^2]^{\mu} \tag{35}$$

we obtain the total loss fraction as

$$L = \frac{\int_0^{\pi}\int_0^1 l(r,\theta)\, s(r)\, r\, dr\, d\theta}{\int_0^{\pi}\int_0^1 s(r)\, r\, dr\, d\theta} = \frac{1}{\pi}\int_0^{\pi}\left[2(\mu+1)\int_0^1 l(r,\theta)\,(1-r^2)^{\mu}\, r\, dr\right] d\theta \tag{36}$$

The present model is primarily intended to describe moderate losses as defined by the condition $r_{bs}>0$. By performing the θ-integration in eq.(36) we obtain

$$L = \frac{1}{\pi}\sqrt{\frac{2}{1+A}}\,\frac{1}{1-r_{bs}}\int_{r_{bs}}^1 (1-r^2)^{\mu+1}\, dr + (1-r_{bs}^2)^{\mu+1}\left(\frac{1}{2} - \frac{1}{\pi}\sqrt{\frac{2}{1+A}}\right) \tag{37}$$

In the region of present interest the last term in eq. (37) due to the passing particles represents a small correction to the total loss fraction and will be neglected. Thus, finally we obtain the following simple expression for the total prompt loss fraction of high energy charged particles in an axisymmetric Tokamak:

$$L \approx \frac{1}{\pi}\sqrt{\frac{2}{1+A}}\,\frac{1}{1-r_{bs}}\int_{r_{bs}}^1 (1-r^2)^{\mu+1}\, dr \tag{38}$$

where r_{bs} is determined by eqs. (26) and (27). Eq. (38) provides a more accurate approximation for the prompt losses than given previously e.g. [9, 10].

4. COMPARISON WITH NUMERICAL RESULTS

To verify the prompt losses predicted by eq. (36) we have made comparisons with the results of numerical simulations produced by CASINO, a code simulation of alpha particle orbits in a axisymmetric Tokamak.

The code is constructed around a core consisting of a particle follower which simulates the particle orbits by using the constants of motion. Under the conditions of an axisymmetric Tokamak model and a time scale much shorter

than the collision times this is a fast and reliable calculation process that does not introduce systematical errors.

In fig. 6 we compare the predictions of eq. (36) with numerical results from the CASINO code for the case A=6, μ=4, n=2, p=1, but for varying total current, I. The agreement is good for currents I>1.5 MA. The critical current when confinement starts to deteriorate is in qualitative agreement with the simple estimate given by eq. (3) (in this case I>1.2 MA).
It is interesting to note that based on our analysis of the orbit dynamics we can define a more accurate condition for good confinement by requiring, cf. eq. (23), $r_{bs} \geq 0$ or equivalently $K_s \geq 1$, cf. Fig. 4. This last condition can be rewritten as

$$I\sqrt{A} > \frac{1+\sqrt{3\left(1+\frac{1}{A}\right)}}{2ZF(1)}\sqrt{ME} \tag{39}$$

which is analogous to eq. (3), but also includes information about the current profile (through F(1)). For a parabolic current profile (F(1)=3/4) the corresponding confinement condition for alpha particles becomes, cf eq.(3)

$$I\sqrt{A} > 3.4 \tag{40}$$

In fact, $r_{bs}=0$ can also be taken as a qualitative limit of validity for the approximate loss analysis as summarized in eq. (36) (note that $r_{bs}=0$ occurs for I=1.5 MA in Fig. 4).
In Fig. 7 we have illustrated the dependence of the loss fraction on the source exponent, μ, for A=4, I=2.8 MA and a parabolic current profile. The source profile, s(r), of the fusion produced particles is determined by the densities, $n_1(r)$ and $n_2(r)$, and the temperature, T(r), of the reacting ions according to

$$s(r) \propto n_1(r)n_2(r)<\sigma v> \propto n_1(r)n_2(r)T^{\gamma}(r) \tag{41}$$

where $<\sigma v>$ denotes the fusion reactivity which has been assumed to scale as $<\sigma v> \propto T^{\gamma}$. This implies that

$$\mu = m_{n_1} + m_{n_2} + \gamma m_T \tag{42}$$

where m_{n_1}, m_{n_2} and m_T denote the corresponding density and temperature profile exponents. For the DT-reaction with T = 10–20 keV we have $\gamma = 2$, which implies that μ tends to be high, e.g. $\mu \geq 4$ where the agreement between the approximation and the CASINO results is seen to be good.

Finally in Fig. 8 we have illustrated the dependence of the loss fraction on the aspect ratio. The agreement between the CASINO results and the approximate loss formula is again g d but begins to deteriorate for iow aspect ratios. However, part of this discrepancy is due to the fact that the current density profile of a true toroidal geometry (as used in the CASINO code) is not symmetric over the cross section as is the current profile used in the approximate analysis.

5. SAWTOOTH-INDUCED LOSSES OF HIGH ENERGY CHARGED PARTICLES

A prominent feature in modern hot Tokamak experiments is the presence of significant sawtooth activity. The characteristic sawtooth variation has been observed in plasma temperature and density but also in signals related to fusion-produced quantities like neutron and high-energy charged particle emission, [11]. However, in addition to the expected sawtooth variation, the emission of fusion produced charged particles also exhibits a particular feature in the form of a high intensity loss burst of short duration during the sawtooth crash. A plausible quantititative explanation of the physical mechanism leading to the loss burst has been given as follows [5]: At, or shortly after the sawtooth crash, temperature, density, and possibly also current profile broaden. The concomitant degradation of confinement releases those particles which have accumulated on confined orbits during the sawtooth rise, but which are transferred into the loss region during the redistribution phase of the sawtooth crash. Since the redistribution time is a small fraction of the accumulation time (being the smaller of the slowing down time and the sawtooth period), the inherent amplification should give rise to a high-intensity burst during the redistribution phase.

The total production rate, S, of the fusion produced particles is given by

$$S = \int_V n_1 n_2 \langle \sigma v \rangle dV \tag{43}$$

where V denotes plasma volume. For simplicity we assume equal ion densities and a power law approximation of the reaction rate, as in eq. (41)

$$\langle \sigma v \rangle \propto T^{\gamma} \tag{44}$$

The space dependence of the density and the temperature is modelled as:

$$n_1 = n_2 = n(0)\left(1-\frac{r^2}{a^2}\right)^{m_n}$$

$$T = T(0)\left(1-\frac{r^2}{a^2}\right)^{m_T} \tag{45}$$

The loss rate, S_l, of charged particles is determined by the local loss fraction, $l(x)$ which implies that

$$S_l \propto n^2 T^{\gamma}(0)\int_0^1 (1-x^2)^{\mu}\, l(x)x\, dx \tag{46}$$

where the source profile exponent, μ, is given by

$$\mu = 2m_n + \gamma m_T$$

Excluding the burst feature, which will be treated separately later, the sawtooth induced change in emission rate is small and can be estimated as follows:

$$\frac{\Delta S_l}{S_l} = 2\frac{\Delta n(0)}{n(0)} + \gamma\frac{\Delta T(0)}{T(0)} + \frac{\Delta M}{M} \tag{47}$$

where

$$M \equiv \int_0^1 (1-x^2)^{\mu}\, l(x)x\, dx \tag{48}$$

and ΔS_l, $\Delta n(0)$, $\Delta T(0)$, and ΔM denote the changes of the corresponding quantities at the sawtooth crash. Since $\Delta n(0)$ and $\Delta T(0)$ are negative whereas $\Delta M > 0$, the last term in eq. (47) tends to counteract the drop in emission rate caused by the two first terms, cf [5]. This is more clearly seen when differentiating eq. (48) to obtain ΔM

$$\Delta M = \Delta\mu\int_0^1 (1-x^2)^{\mu}\ln(1-x^2)\, l(x)x\, dx + \int_0^1 (1-x^2)^{\mu}\,\Delta l(x)x\, dx \tag{49}$$

where $\Delta\mu<0$ and $\Delta l(x)>0$ denote the changes in source profile exponent and local loss rate respectively.

Using the approximate expression for the loss fraction according to eq. (38) we find

$$M \propto \frac{1}{1-r_{bs}} \int_{r_{bs}}^{1} (1-x^2)^{\mu+1} dx \tag{50}$$

which implies

$$\frac{\Delta M}{M} \approx G(\mu, r_{bs})\,\Delta\mu + H(\mu, r_{bs}) \frac{\Delta r_{bs}}{1-r_{bs}} \tag{51}$$

where

$$G(\mu, r_{bs}) = \frac{\int_{r_{bs}}^{1} (1-x^2)^{\mu+1} \ln(1-x^2)\, dx}{\int_{r_{bs}}^{1} (1-x^2)^{\mu+1} dx}$$

$$H(\mu, r_{bs}) = 1 - \frac{(1-r_{bs})\,(1-r_{bs}^2)^{\mu+1}}{\int_{r_{bs}}^{1} (1-x^2)^{\mu+1} dx}$$

Simple area considerations show that $H(\mu, r_{bs})<0$ and since also $\Delta r_{bs}<0$, each of the differential contributions to ΔM are positive.

Assuming negligible background particle and energy losses during the sawtooth crash, cf [5], we find

$$\Delta m_n = (m_n+1) \frac{\Delta n(0)}{n(0)}$$

$$\Delta m_T = m_T \frac{\Delta n(0)}{n(0)} + (m_T + m_n + 1) \frac{\Delta T(0)}{T(0)} \tag{52}$$

which implies

$$\Delta\mu = [2(m_n+1) + \gamma m_T] \frac{\Delta n(0)}{n(0)} + \gamma (m_T + m_n + 1) \frac{\Delta T(0)}{T(0)} \tag{53}$$

The change in r_{bs} can be related to the change in current profile, cf. eq. (26). For the present purpose it is sufficient to use the simpler approximation $r_{bs} = 1-1/K_s$ which implies

$$\Delta r_{bs} = (1-r_{bs}) \frac{\Delta F(1)}{F(1)} \tag{54}$$

and for current profiles $j(r) \sim (1-x^2)^p$ it can be shown, see appendix

$$F(1) = \frac{1}{2}[C + \Psi(p+2)] \tag{55}$$

where $C \sim 0.577$ is the Euler constant and $\Psi(x) = d\ln\Gamma(x)/dx$ is the logarithmic derivative of the Gamma function $\Gamma(x)$.

As is also shown in the appendix, the value of the axial safety factor q(0) satisfies

$$q(0) \propto \frac{1}{p+1} \tag{56}$$

Thus we have

$$\frac{\Delta r_{bs}}{1-r_{bs}} = \frac{\Delta F(1)}{F(1)} \approx -\frac{p+1}{C+\Psi(p+2)} \frac{d\Psi(p+2)}{dp} \frac{\Delta q(0)}{q(0)} \tag{57}$$

Finally, collecting the results we obtain for the change in loss rate

$$\frac{\Delta S_l}{S_l} = \{2 + [2(m_n+1) + \gamma m_T]\, G(\mu, r_{bs})\} \frac{\Delta n(0)}{n(0)} +$$

$$+ \gamma\{1 + (m_T + m_n + 1)\, G(\mu, r_{bs})\} \frac{\Delta T(0)}{T(0)} -$$

$$- H(\mu, r_{bs}) \frac{p+1}{C+\Psi(p+2)} \frac{d\Psi(p+2)}{dp} \frac{\Delta q(0)}{q(0)} \tag{58}$$

In order to simplify the analysis of the loss burst feature we will make two assumptions: (i) the sawtooth period, t_s, is much smaller than the slowing down time, τ_s, of the high energy ions, implying that the distribution function can be considered monoenergetic and (ii) the sawtooth crash makes the distribution function of the accumulating particles isotropic also at radii, $r > r_{bs}$, where velocity space loss regions exist during the sawtooth build up

phase. This latter assumption is supported by the emerging evidence that high energy charged particles are more strongly affected by sawteeth than thermal particles, [12].

Consider high energy particles produced at a rate given by eq. (43) and accumulating on confined orbits during a sawtooth period, t_s. During the sawtooth crash and redistribution phase, lasting a time $t_r << t_s$, some of these particles are assumed to be transferred to unconfined orbits by the combined effects of (i) velocity space isotropization, (ii) a broadening of the density of the accumulated particle, and (iii) an increasing local loss fraction. An estimate of the magnitude of the loss burst intensity, S_l^{burst} relative to the background loss intensity can then be given as

$$\frac{S_l^{burst}}{S_l} \approx \frac{t_s}{t_r} \frac{\int_0^1 (1-x^2)^{\mu'} l'(x) x\, dx}{\int_0^1 (1-x^2)^{\mu} l(x) x\, dx} \tag{59}$$

where the density of the accumulated fast particles $n_f(r)$ is assumed to be of the form $n_f(r)=n_f(0)(1-r^2/a^2)^{\mu}$ and prime denotes values after the crash. Assuming a redistribution which preserves the total number of particles (in the absence of losses) we have

$$\mu' = (\mu+1)\frac{n_f'(0)}{n_f(0)} - 1 \tag{60}$$

and using our simplified loss formula we obtain

$$\frac{S_l^{burst}}{S_l} \approx \frac{t_s}{t_r} \frac{\int_{x_{bs}'}^1 (1-x^2)^{(\mu+1)n'(0)/n(0)}\, dx}{\int_{x_{bs}}^1 (1-x^2)^{\mu+1}\, dx} \tag{61}$$

As an application we consider the losses of 3.5 MeV alpha particles produced by a thermal DT plasma at temperatures T≈20 keV where $\gamma \approx 2$. The density and temperature profiles are characterized by $m_n=0.5$ and $m_T=1$ i.e. $\mu=3$. Furthermore, assume a parabolic current profile (p=1) and a situation where $r_{bs}=r_{bs}'=0$. Then the regular change in loss rate can be written

$$\frac{\Delta S_l}{S_l} \approx 1.1\left(\frac{\Delta n(0)}{n(0)} + \frac{\Delta T(0)}{T(0)}\right) + 0.8\,\frac{\Delta q(0)}{q(0)} \tag{62}$$

The density drop on axis can be expected to be rather small typically -(2-5)%, cf. [13], whereas the ion temperature drop tends to be significantly higher, say -(10-20)%, cf. [13]. The change in safety factor on axis should be positive and recent measurements on JET give typical values of $\Delta q(0)/q(0) \approx (2\text{–}5)\%$, cf.[14]. Thus we conclude that the regular change in the loss rate of the high energy alpha particles should be comparable to the ion temperature drop.

The situation is drastically different for the burst intensity. Even in the case when no profile broadening in space occurs, i.e. $n_j(0)=n_j'(0)$, the velocity space scrambling of the pitch angles gives rise to a relative burst intensity $S_l^{burst}/S_l=t_s/t_r>>1$.. The ratio t_s/t_r in a future fusion plasma is difficult to predict, but for the proton bursts observed on JET, [11], this ratio is typically $t_s/t_r \sim 100/10=10$.

Using again our simplified loss formula we can estimate the burst intensity in a general case (for $r_{bs}=0$) with density redistribution as

$$\frac{S_l^{burst}}{S_l} \approx \frac{t_s}{t_r}\Lambda(\xi) \tag{63}$$

where

$$\Lambda(\xi)=\frac{\int_0^1 (1-x^2)^{\xi(\mu+1)}\,dx}{\int_0^1 (1-x^2)^{\mu+1}\,dx}=\frac{\Gamma(\xi(\mu+1)+1)\,\Gamma\left(\mu+\frac{5}{2}\right)}{\Gamma\left(\xi(\mu+1)+\frac{3}{2}\right)\Gamma(\mu+2)} \tag{64}$$

The parameter ξ is defined by

$$\xi \equiv \frac{n_f'(0)}{n_f(0)}$$

The redistribution of high energy alphas during a sawtooth crash is also difficult to predict. However, present day experimental evidence e.g. [12] indicate that high energy ions may be more susceptible to sawtooth crashes than thermal ions. On the other hand the characteristic function $\Lambda(\xi)$ does not vary significantly cf Fig. 9 and the magnitude of the loss burst primarily reflects the ratio of the sawtooth period to the redistribution time.

6. CONCLUSIONS

Based on an axisymmetric Tokamak model with cicular cross-section a simple and useful formula for the fraction of promptly lost high energy particles has been derived. The predicted losses as function of total plasma current, aspect ratio and source profile exponent have been investigated and compared with corresponding numerical simulations by the CASINO code. The analytical and numerical results are in good agreement in parameter regions of physical and practical interest. Deviations occur mainly for large particle losses and for low aspect ratios when the inherent shortcoming of the circular Tokamak model becomes important.

The approximate expression for the particle loss fraction is used to analyze the variation of alpha particle losses in the presence of sawtooth activity. It is found that two types of changes in the loss rate can be expected at the sawtooth crash: (i) a regular change which should be comparable to the ion temperature drop and (ii) a loss burst feature when particles, wich have been accumulating during the sawtooth rise, are transformed to unconfined orbits. The loss burst intensity is mainly determined by the ratio of sawtooth period to redistribution time.

APPENDIX

The purpose of this appendix is to give a more detailed presentation of the analysis relating the value of the normalized flux function at the plasma boundary, F(1), to the axial value of the safety factor, q(0).

We will restrict our analysis to current profiles of the form $J(r) \sim J_o(1-r^2/a^2)^p$, in which case F(1) becomes

$$F(1) = \frac{\sum_{j=0}^{p} \frac{(-1)^j}{(2j+2)^2} \binom{p}{j}}{\sum_{j=0}^{p} \frac{(-1)^j}{2j+2} \binom{p}{j}} \tag{A1}$$

In order to rewrite F(1) we consider the identity

$$(1-x^2)^p = \sum_{j=0}^{p} (-1)^j x^{2j} \binom{p}{j} \tag{A2}$$

This implies that

$$x\,(1-x^2)^p = \sum_{j=0}^{p} (-1)^j x^{2j+1} \binom{p}{j} \tag{A3}$$

Integrating eq. (A3) from 0 to x we obtain

$$\frac{1}{2(p+1)} [1-(1-x^2)^{p+1}] = \sum_{j=0}^{p} \frac{(-1)^j}{2j+2} x^{2j+2} \binom{p}{j} \tag{A4}$$

In particular, for x=1 we identify the nominator in eq. (A1) as

$$\sum_{j=0}^{p} \frac{(-1)^j}{2j+2} \binom{p}{j} = \frac{1}{2(p+1)} \tag{A5}$$

We proceed further by dividing eq. (A4) with x and integrating from 0 to 1. This yields the denominator in eq. (A1) as

$$\sum_{j=0}^{p} \frac{(-1)^j}{(2j+2)^2} \binom{p}{j} = \frac{1}{2(p+1)} \int_0^1 \frac{1}{x} [1-(1-x^2)^{p+1}]\, dx =$$

$$= -\frac{1}{4} \int_0^1 (1-t)^p \ln(t)\, dt = -\frac{1}{4(p+1)} [C+\Psi(p+2)] \qquad (A6)$$

where $\psi(x)$ is the logarithmic derivative of the Gamma function and $C=-\psi(1)=0.577$ is Euler's constant. Thus, F(1) can be written as

$$F(1) = \frac{1}{2} [C+\Psi(p+2)] \qquad (A7)$$

The safety factor, q(r), is defined as

$$q(r) = \frac{rB(0)}{RB_p(r)} \qquad (A8)$$

where the poloidal magnetic field, $B_p(r)$, is linked to the current profile, J(r), by the relation

$$B_p(r) = \frac{\mu_o J_o a^2}{r} \Phi\left(\frac{r}{a}\right) \qquad (A9)$$

where

$$\Phi(x) = \int_0^x x\,(1-x^n)^p\, dx \qquad (A10)$$

The total current, I, is

$$I = \iint J\, dS = 2\pi J_o a^2 \Phi(1) \qquad (A11)$$

and consequently

$$q(r) = \frac{2\pi a^2 B}{\mu_o RI} \frac{\frac{r^2}{a^2}\Phi(1)}{\Phi\left(\frac{r}{a}\right)} \qquad (A12)$$

Since $\Phi(x) \sim 1/2\ x^2$ irrespective of n and p we obtain

$$q(0) = 2A\,\Phi(1) \tag{A13}$$

where

$$A = \frac{2\pi a^2 B}{\mu_o R I} \tag{A14}$$

Again we assume n = 2, in which case $\Phi(1)$ becomes particularly simple, viz.

$$\Phi(1) = \frac{1}{2(p+1)} \tag{A15}$$

and

$$q(0) = \frac{A}{p+1} \tag{A16}$$

Since the total current remains constant during the sawtooth crash we obtain by differentiation

$$\frac{\Delta q(0)}{q(0)} = -\frac{\Delta p}{p+1} \tag{A17}$$

Differentiating eq. (A7) we obtain

$$\Delta F(1) = \frac{1}{2}\,\psi'(p+2)\,\Delta p \tag{A18}$$

and eliminating Δp we finally have

$$\Delta F(1) = -\frac{p+1}{2}\,\psi'(p+2)\,\frac{\Delta q(0)}{q(0)} \tag{A19}$$

REFERENCES

[1] J.A. Rome, D.G. McAlees, J.D. Callen, R.H. Fowler, Nucl. Fus. 16 (1976), 55.

[2] D. Andersson, H. Hamnen, and M. Lisak, CTH-/EFT/PP-1989-03 (1989).

[3] W. Bauer, K.L. Wilson, C.L. Bisson, L.G. Haggmark, and R.J. Goldston, Nucl. Fus. 19 (1979), 93.

[4] W.W. Heidbrink, R.E. Chrien, J.D. Strachan, Nucl. Fus. 23 (1983), 917.

[5] D.F.H. Start et al 17th EPS Conference on Controlled Fusion and Plasma Heating, Amsterdam, 25-29 June 1990, paper F8.

[6] D. Anderson and M. Lisak, Plasma Physics 32 (1990), 141.

[7] S.J. Zweben, R.L. Boivin, M. Diesso, S. Hayes, H.W. Hendel, H. Park,J.D. Strachan, Nucl. Fus. 30 (1990) 1551.

[8] M. Ohnishi, N. Ao, and J. Wakabayashi, Nucl. Fus. 18 (1978) 859.

[9] Yu. Kolesnichenko, Nucl. Fus. 20 (1980), 727.

[10] D. Anderson and P. Batistoni, Nucl. Fus. 28 (1988), 2151

[11] G. Martin, O. Jarvis, J. Källne, V. Merlo, G. Sadler, and P. Van Belle, Physica Scripta T16 (1987), 171.

[12] F.B. Marcus et al 17th EPS Conf., Amsterdam (1990).

[13] P. Batistoni, M. Rapisarda, and D. Anderson, Nucl. Fus. 30 (1990), 625.

[14] J. O'Rourke, JET-P (90) 43.

FIGURE CAPTIONS

Fig. 1. Simulation of orbits for alpha particles with the same energy and birth point but for different pitch angles (from the CASINO code).

Fig. 2. Numerical calculation of loss regions (adapted from [1]).

Fig. 3. Qualitative model of loss region (adapted from [10]).

Fig. 4. The critical radius r_{bs} as a function of K_s.

Fig. 5. F(1) as a function of current profile exponent p for n=2. (Note that $K_s \sim F(1)$)

Fig. 6. Loss fraction as a function of total current (A=6, μ=6, n=2, p=1).

Fig. 7. Loss fraction as function of the source profile exponent μ (A=4, I=2.8 MA, n=2, p=1).

Fig. 8. Loss fraction as function of the aspect ratio (μ=6, I=2.2 MA, n=2, p=1).

Fig. 9. The characteristic function $\Lambda(\xi)$ which determines the ratio of burst intensity to loss rate during redistribution time (μ=3).

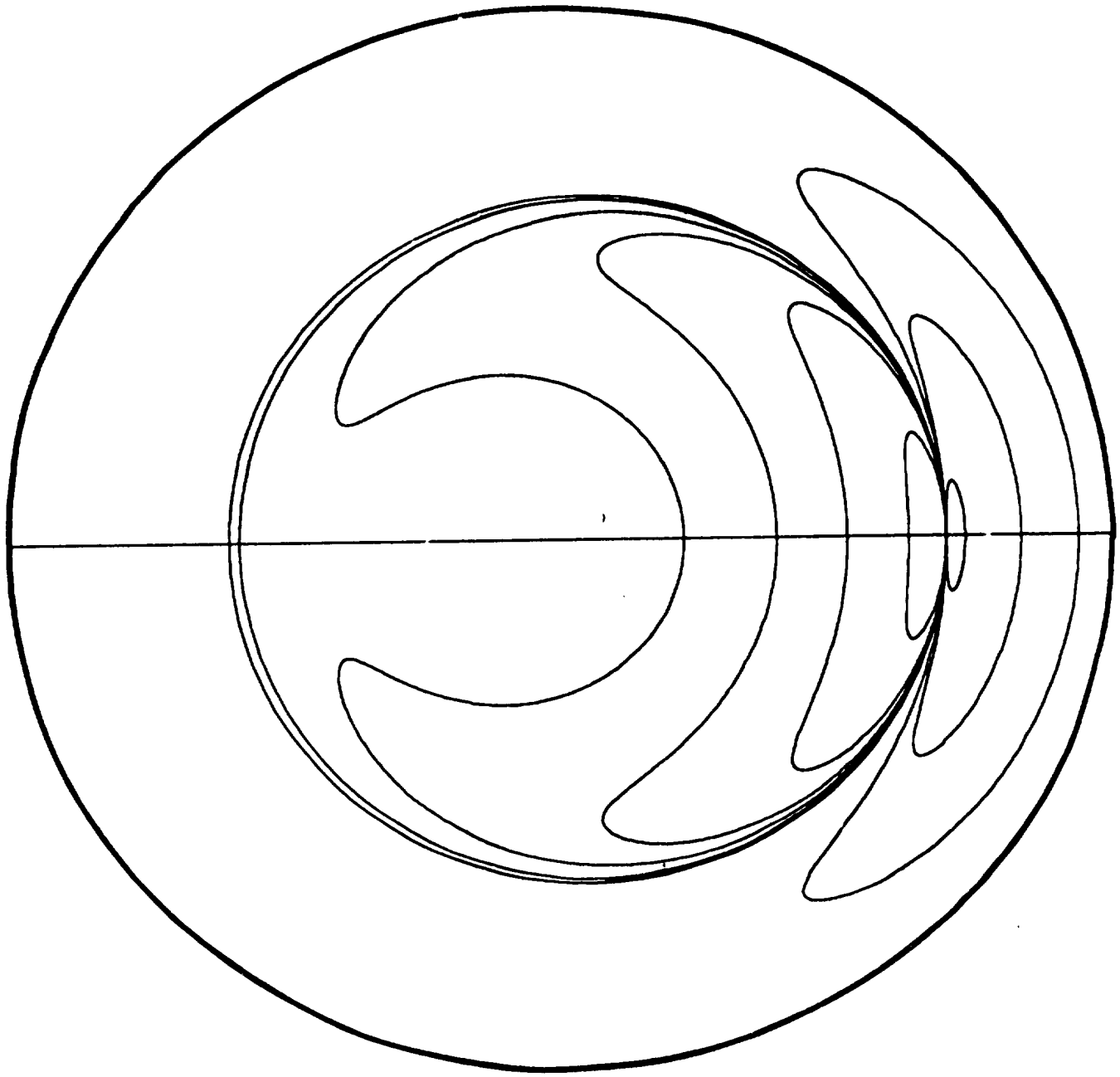

Fig. 1

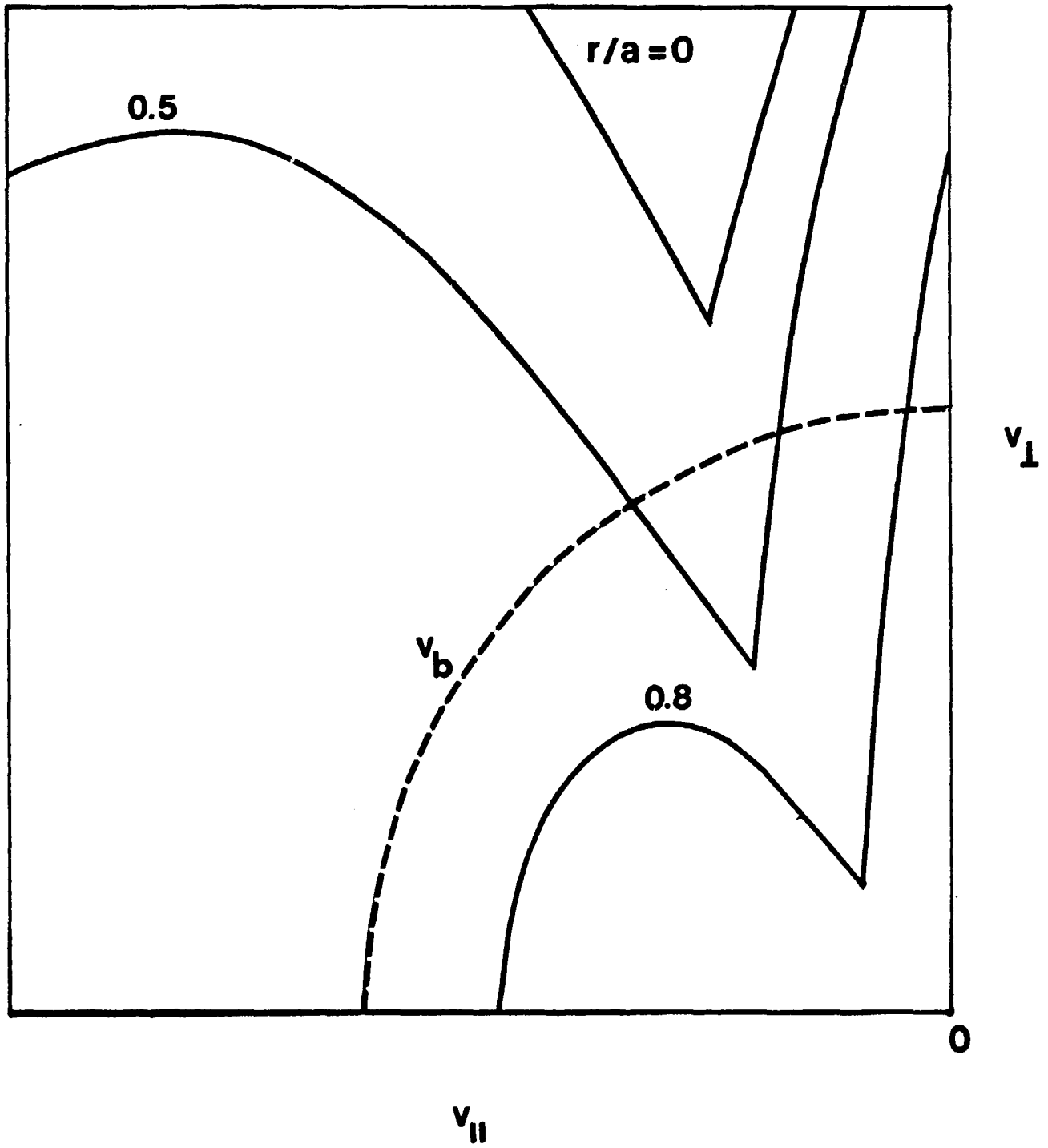

Fig. 2

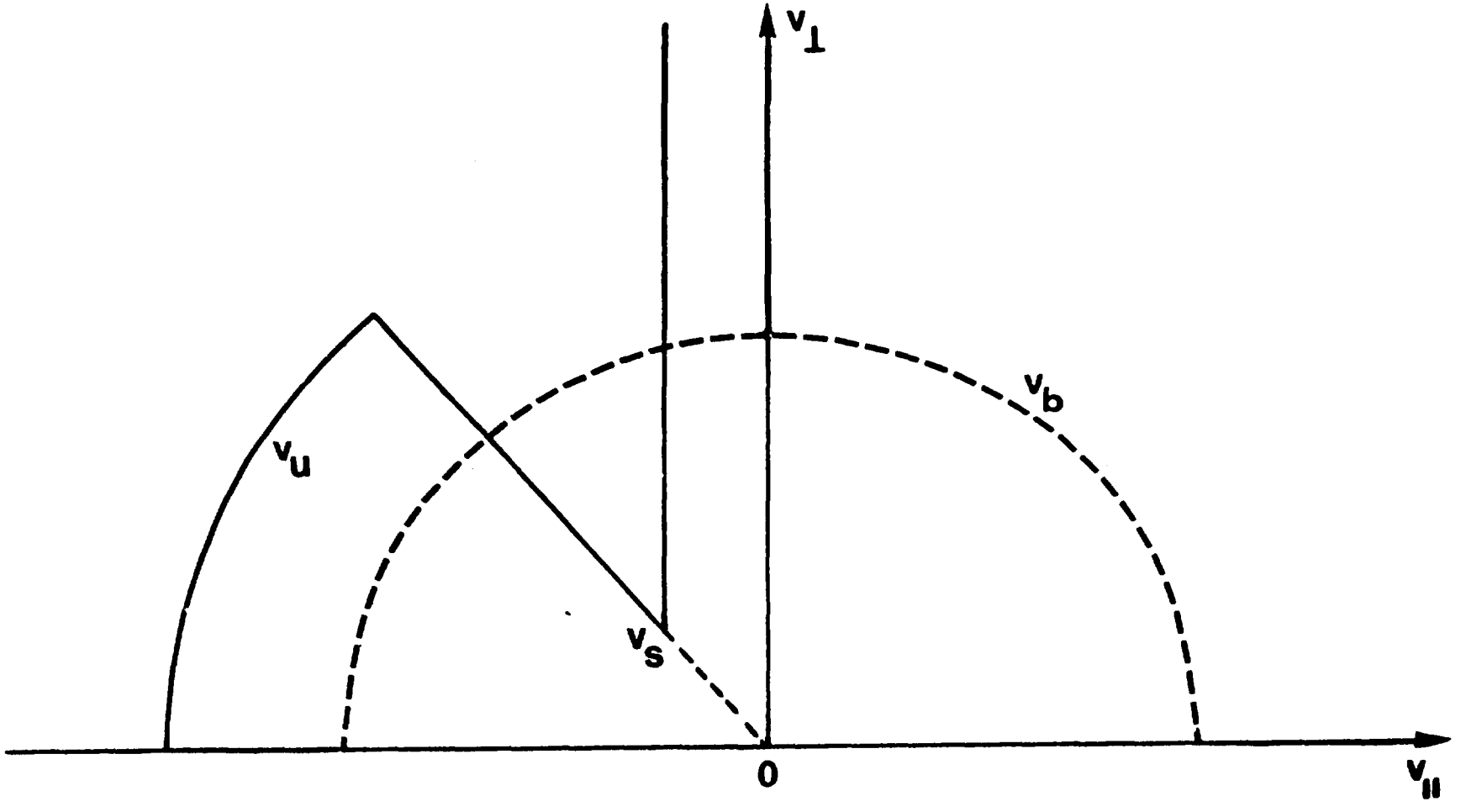

Fig. 3

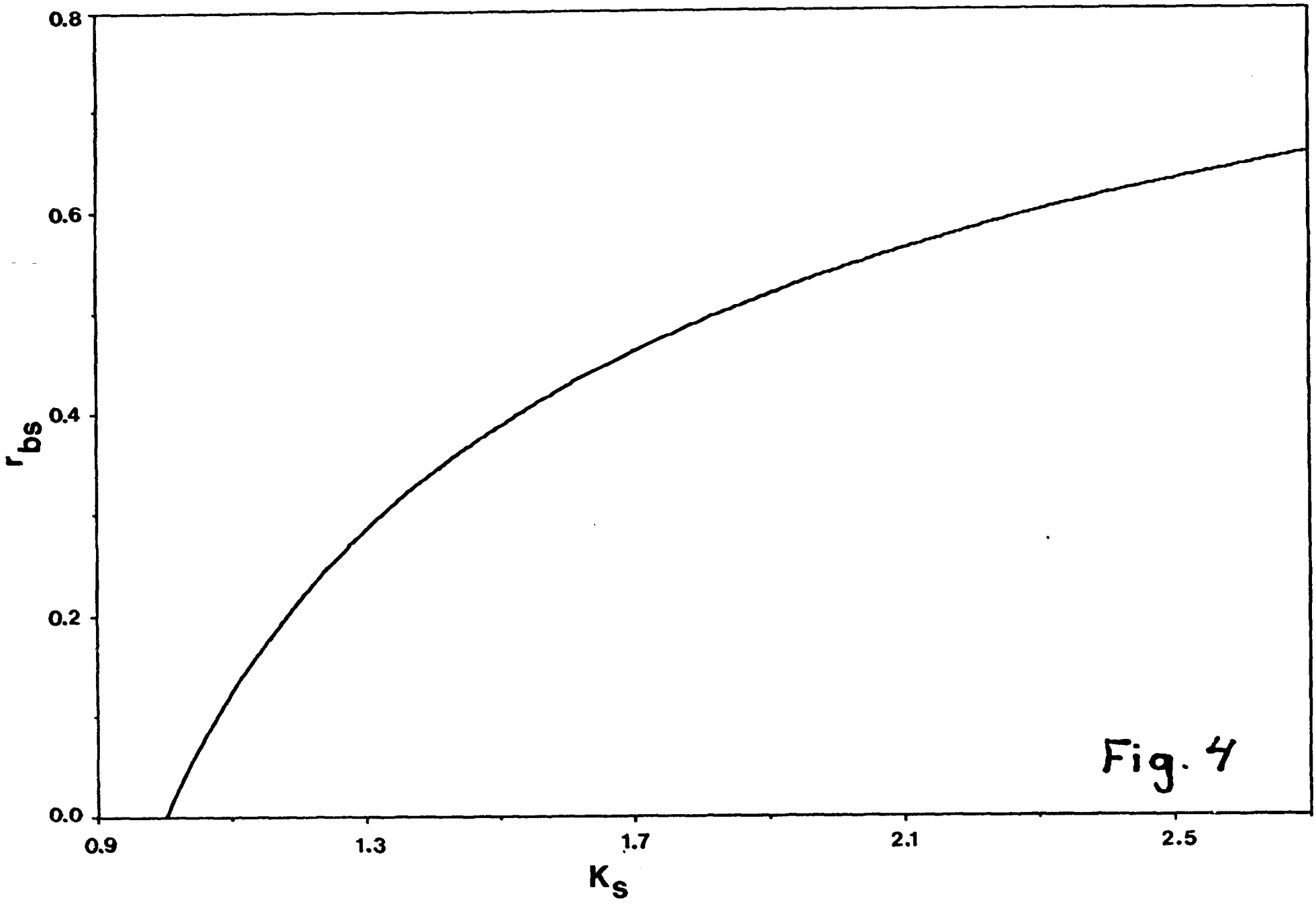

Fig. 4

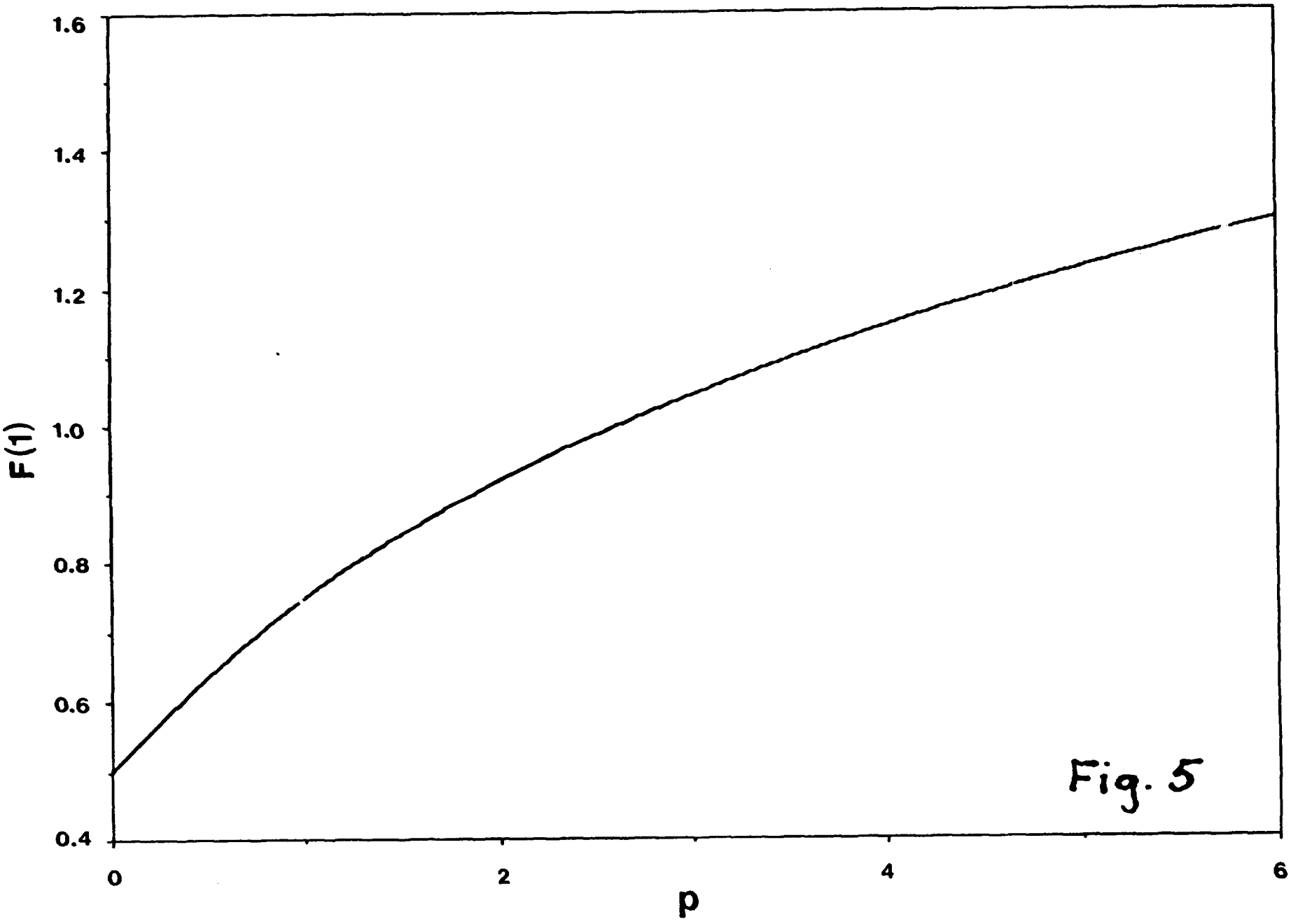

Fig. 5

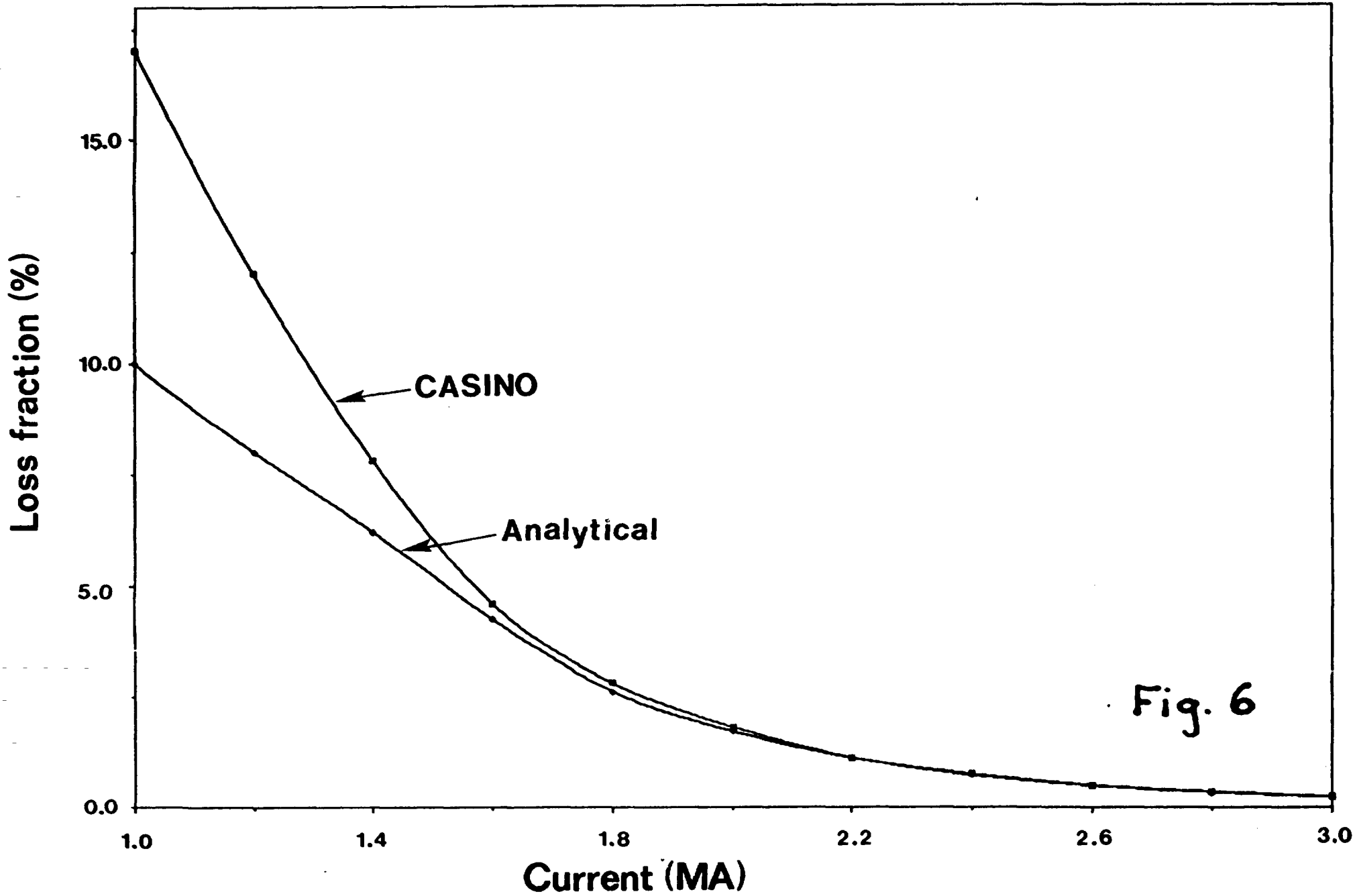
15.0
10.0
5.0
0.0
Loss fraction (%)
CASINO
Analytical
1.0
1.4
1.8
2.2
2.6
3.0
Current (MA)

Fig. 6

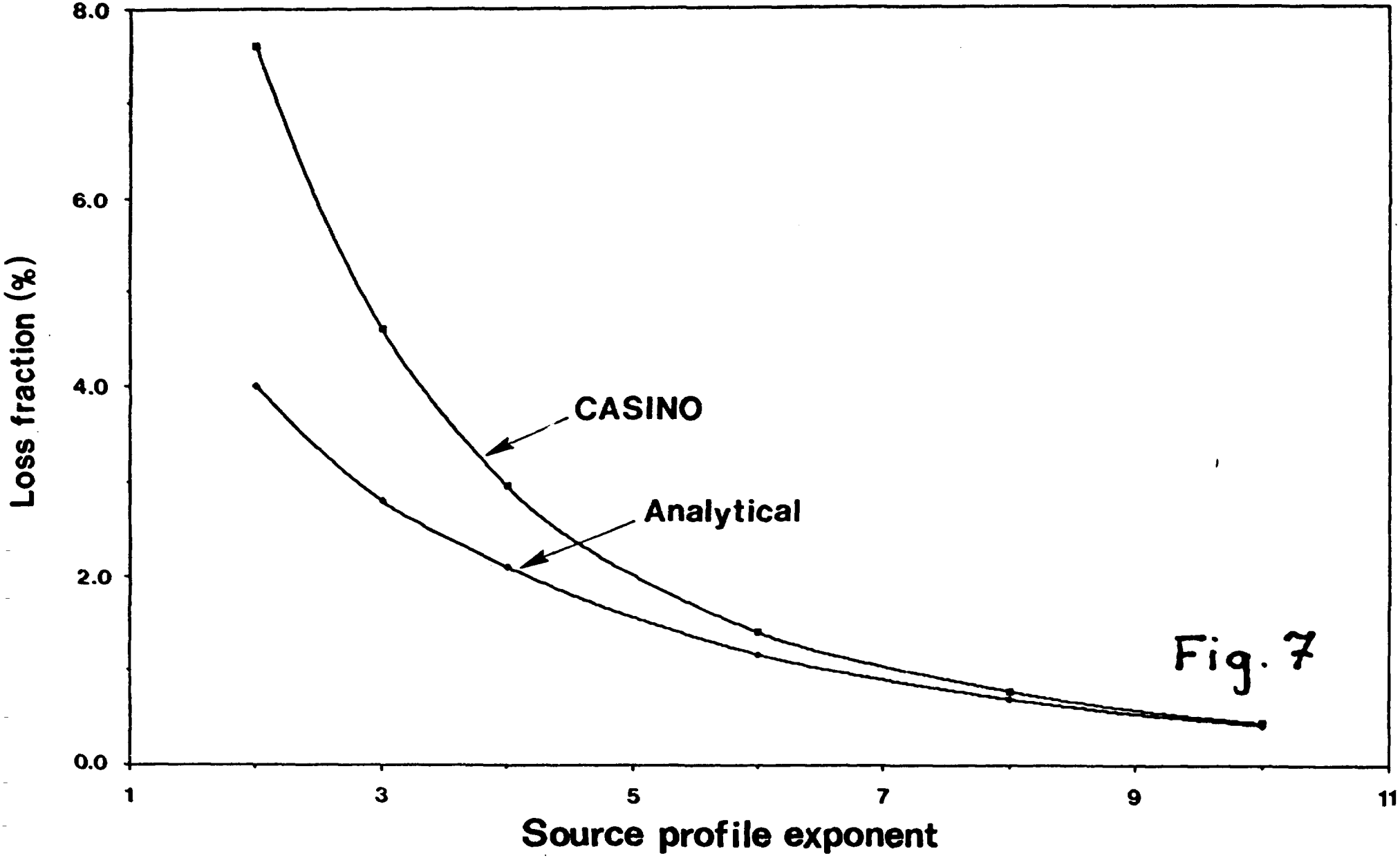
8.0
6.0
4.0
2.0
0.0
Loss fraction (%)
CASINO
Analytical
1
3
5
7
9
11
Source profile exponent

Fig. 7

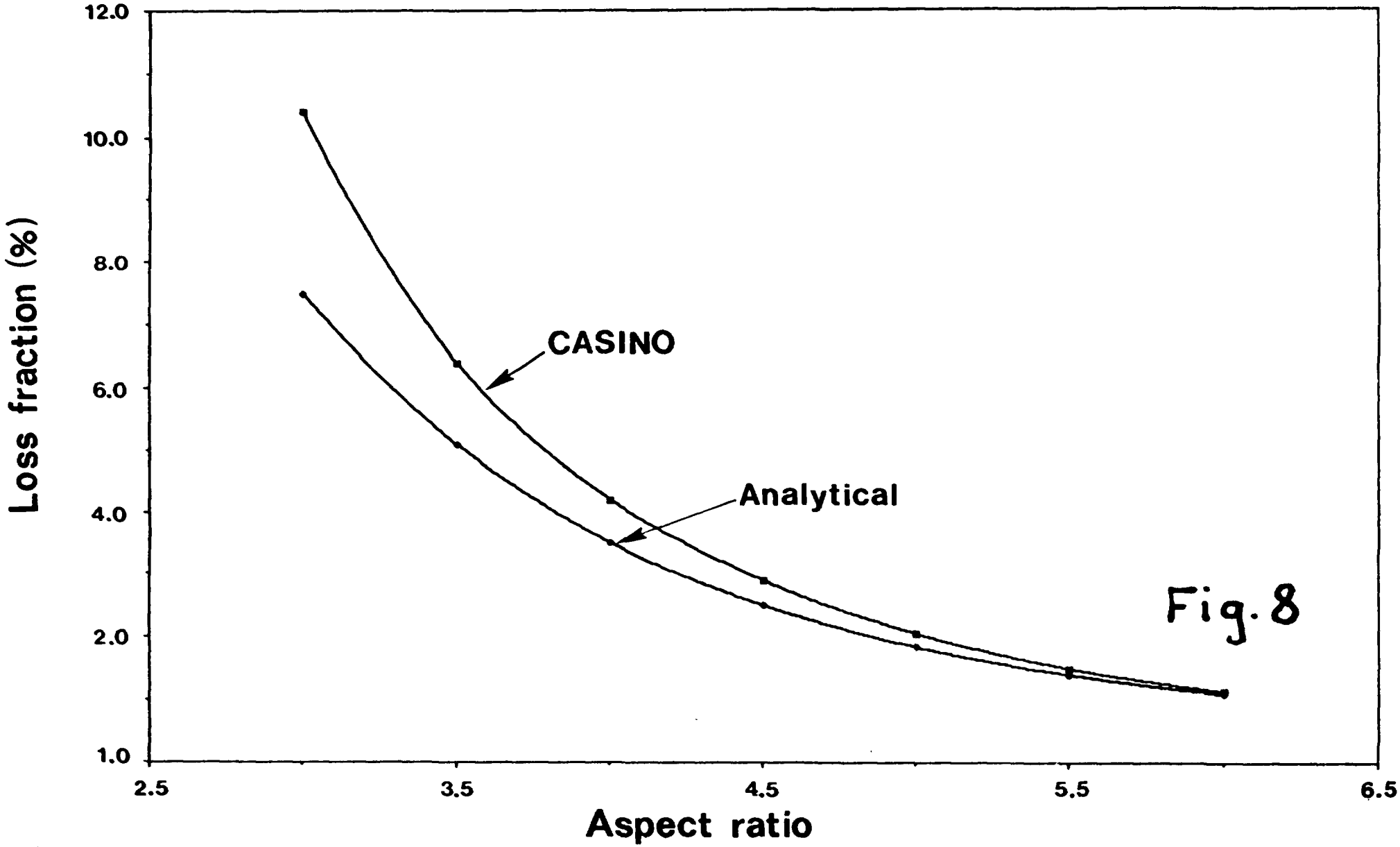
12.0
10.0
8.0
6.0
4.0
2.0
1.0
Loss fraction (%)
CASINO
Analytical
2.5
3.5
4.5
5.5
6.5
Aspect ratio

Fig. 8

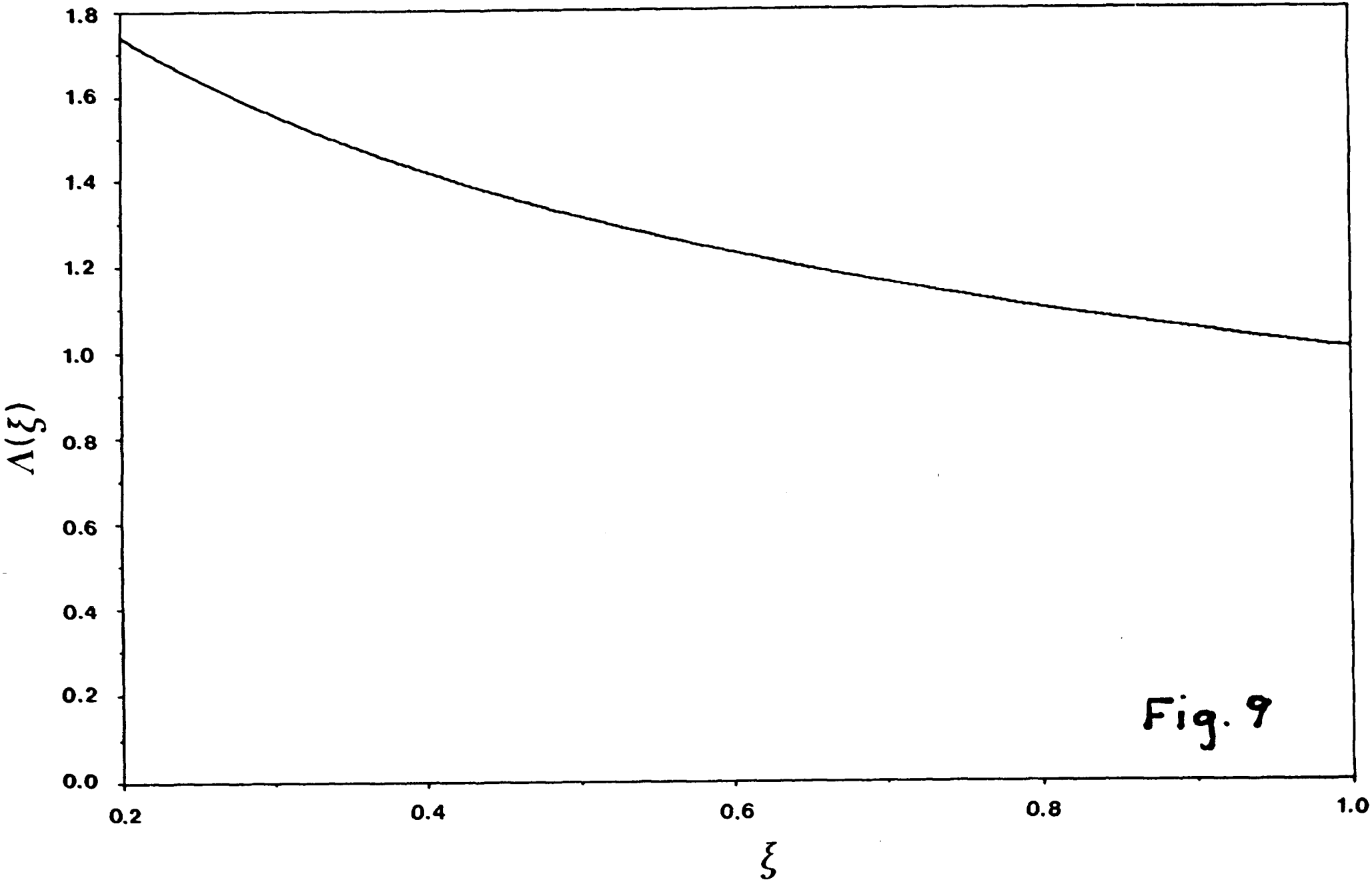

Fig. 9